Theoretical Analysis and Performance of OFDM Signals in Nonlinear AWGN Channels

Paolo Banelli, *Member, IEEE*, and Saverio Cacopardi, *Member, IEEE*

***Abstract*—Orthogonal frequency-division multiplexing (OFDM) baseband signals may be modeled by complex Gaussian processes with Rayleigh envelope distribution and uniform phase distribution, if the number of carriers is sufficiently large. The output correlation function of instantaneous nonlinear amplifiers and the signal-to-distortion ratio can be derived and expressed in an easy way. As a consequence, the output spectrum and the bit-error rate (BER) performance of OFDM systems in nonlinear additive white Gaussian noise channels are predictable both for uncompensated amplitude modulation/amplitude modulation (AM/AM) and amplitude modulation/pulse modulation (AM/PM) distortions and for ideal predistortion. The aim of this work is to obtain the analytical expressions for the output correlation function of a nonlinear device and for the BER performance. The results in closed-form solutions are derived for AM/AM and AM/PM curves approximated by Bessel series expansion and for the ideal predistortion case.**

***Index Terms*—Communication system nonlinearities, complex gaussian processes, nonlinear distortions, OFDM, predistortion.**

I. Introduction

ADSL (asymmetric digital subscriber line) [1], DAB (digital audio broadcasting) [2], and DVB-T (digital video broadcasting-terrestrial) [3] are emerging telecommunication systems that make use of the orthogonal frequency-division multiplexing (OFDM) technique. The OFDM signal, carried by a large number of carriers, is very sensitive to nonlinear distortions because of its greatly variable envelope, which depends on the instantaneous phase value of each carrier. Due to the central limit theorem, the complex baseband OFDM signal can be modeled (for a high number of independently modulated carriers) like a complex Gaussian process with Rayleigh envelope distribution. This allows the analytical treatment of nonlinear OFDM systems making use of the more general results for nonlinear distortions of Gaussian signals.

Analog-to-digital (A/D) converters, mixers, and power amplifiers are usually the major sources of nonlinear distortions due to the limited range that they allow for signal dynamics. It is possible to distinguish between two different classes of nonlinear distortions: the first, hereafter named Cartesian, acts separately on the baseband components of the complex signal, while the second acts on the envelope of the complex signal. A/D distortions, called Cartesian clipping, belong to the first class, while AM/AM (amplitude distortion which depends on the amplitude of the input) and AM/PM (phase distortion which depends on the amplitude of the input) introduced by power amplifiers belong to the second class.

In the following sections, we will concentrate our analysis on nonlinear distortions introduced by power amplifiers on Gaussian signals, in order to obtain an analytical expression of the output correlation function for envelope nonlinear devices. By using the Fourier transformation, the output correlation function can provide information on the output power spectral density (PSD), and at the same time, it allows the analytical calculation of the output signal-to-nonlinear noise ratio. In this way, it is possible to evaluate the system degradation both for adjacent channel spectral regrowth and bit-error rate (BER) performance in additive white Gaussian noise (AWGN) channels.

Original results will be shown for AM/AM and AM/PM nonlinearities expressed by Bessel series expansion and for the envelope clipping, which represents the ideal precorrection situation. It is worth bearing in mind that the results hold for any input signal that can be modeled as a complex zero-mean Gaussian process (e.g. downlink signals for multiuser CDMA systems).

II. Theoretical Background

The statistical properties of signals that pass through nonlinear devices have been widely investigated in the past [4]–[11].

In [8], the signal-to-noise ratio (SNR) at the output of real nonlinear devices is derived by making use of the Bussgang theorem. The Bussgang theorem for real functions [12] gives the separateness of a nonlinear output as the sum of a useful attenuated input replica and an uncorrelated nonlinear distortion, expressed by

$$s_d(t) = s_u(t) + n_d(t) = \alpha \cdot s(t) + n_d(t) \tag{1}$$

with $s(t)$ being the input signal and $s_u(t)$ and $n_d(t)$, respectively, the useful and distorted part of the output signal $s_d(t)$. The same conclusions can be extended to complex nonlinear distortions represented by the combination of AM/AM and AM/PM nonlinearity [9].

If $f(r) = h(r) \cdot e^{j\phi(r)}$ is a complex nonlinear distortion function, which only depends on the envelope $r(t)$ of the input signal $s(t)$, then the output signal can be expressed by (2). $h(r)$ and

Paper approved by B. L. Hughes, the Editor for Theory and Systems of the IEEE Communications Society. Manuscript received August 24, 1998; revised August 1, 1999.

The authors are with the Department of Electronic and Information Engineering, University of Perugia, 06126 Perugia, Italy (e-mail: banelli@diei.unipg.it; cacopardi@diei.unipg.it).

Publisher Item Identifier S 0090-6778(00)02272-8.

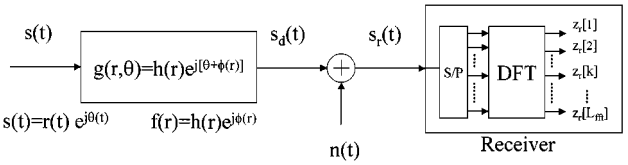

Fig. 1. Nonlinear device in AWGN channels.

$\phi(r)$, respectively, represent the AM/AM and the AM/PM nonlinearity, while $g[\cdot]$ is the nonlinear input–output relationship, as pointed out in Fig. 1.

$$\begin{aligned} s_d(t) &= g[s(t)] \\ &= g[r(t)e^{j\theta(t)}] \\ &= h[r(t)] \cdot e^{j[\theta(t)+\phi[r(t)]]} \\ &= f[r(t)] \cdot e^{j\theta(t)}. \end{aligned} \tag{2}$$

The complex version of the Bussghang theorem allows expressing the output correlation function by (3).

$$R_{s_d s_d}(\tau) = |\alpha|^2 \cdot R_{ss}(\tau) + R_{n_d n_d}(\tau). \tag{3}$$

The complex α attenuation coefficient of the useful component is given by

$$\begin{aligned} \alpha &= \frac{R_{S_d S}(0)}{R_{SS}(0)} \\ &= \frac{E\{s_d^*(t)s(t)\}}{2\sigma^2} \\ &= \frac{E\{f(r)r\}}{2\sigma^2} \\ &= \frac{1}{2\sigma^2} \int_0^\infty f(r) \cdot r \cdot p(r)\, dr \end{aligned} \tag{4}$$

where $R_{S_d S}(\tau)$ denotes the complex input–output cross-correlation function, $f(r)$ represents the nonlinear distorting function, $2\sigma^2$ the input signal power, $p(r)$ the Rayleigh probability density function (pdf) of the input envelope, and $E\{\cdot\}$ the statistical expectation operator.

It is thus possible to compute the output signal-to-nonlinear noise ratio as the power ratio between the two uncorrelated output components by the following expression:

$$\begin{aligned} (\mathrm{SNR})_d &= \frac{R_{s_u s_u}(0)}{R_{n_d n_d}(0)} \\ &= \frac{|\alpha|^2 \cdot R_{ss}(0)}{R_{s_d s_d}(0) - |\alpha|^2 \cdot R_{ss}(0)} \\ &= \frac{|\alpha|^2 \cdot 2\sigma^2}{R_{s_d s_d}(0) - |\alpha|^2 \cdot 2\sigma^2} \end{aligned} \tag{5}$$

However, (5) is not the correct expression of the signal-to-nonlinear noise ratio that degrades the system performance, because the nonlinear distortion noise $n_d(t)$ is distributed over a wider bandwidth than the signal $s(t)$. Moreover, this approach does not permit derivation of the output correlation function and the PSD for the output signal. Different approaches may be used to compute the output correlation function for nonlinear distortions of Gaussian input signals, including the direct method, the transform method, or the derivative method [10], [11]. In this paper, we employ the direct method, based on the classical definition of the output correlation function, by which (see Appendix I) it is possible to prove for any $f(r)$ nonlinear distortion function that expression (2) can be reduced to

$$\begin{aligned} R_{s_d s_d}(\tau) &= \sum_{n=0}^{\infty} c_n \left[\frac{R_{ss}(\tau)}{2\sigma^2}\right]^{2n+1} \\ &= \frac{c_0}{(2\sigma^2)} R_{ss}(\tau) + \sum_{n=1}^{\infty} c_n \left[\frac{R_{ss}(\tau)}{2\sigma^2}\right]^{2n+1} \end{aligned} \tag{6}$$

with $c_n$expressed by

$$\begin{aligned} c_n = \frac{1}{2\sigma^2}\, \frac{1}{n+1} \\ \cdot \left\| \int_{D(r)} f(r) \cdot \frac{r^2}{\sigma^2} \cdot e^{r^2/2\sigma^2} \cdot L_n^{(I)}\left(\frac{r^2}{2\sigma^2}\right) dr \right\|^2 \end{aligned} \tag{7}$$

where $D(r) = \{r\colon 0 \le r \le \infty\}$ is the domain of integration and $L_n^{(k)}(x)$ is the Laguerre function expressed by

$$L_n^{(k)}(x) = \frac{x^{-k}e^x}{n!}\left(\frac{d}{dx}\right)^n (x^{n+k} \cdot e^{-x}). \tag{8}$$

Expressions (6) and (7) were also derived in [5] in relation to the decomposition of nonlinear outputs as sum of uncorrelated terms. The application of (6) and (7) to nonlinear distortion of an OFDM signal proposed in this paper is new, as well as the closed form solution of the integral in (7) when the nonlinear distortion $f(r)$ is expressed by Bessel series expansion or when it is reduced to the soft-limiting of the signal envelope.

It is noteworthy that expression (6) represents the expansion of expression (3), with $c_0/2\sigma^2$ equal to the $|a|^2$ attenuation of the useful signal power and the series representing the correlation function $R_{n_d n_d}(\tau)$ for the nonlinear distortion noise. This expression has a simple physical interpretation. In fact, the Fourier transform of the nth term in the series represents the part of the output PSD $S_{s_d s_d}(v)$ obtained by a $(2n+1)$th convolution of the input PSD with itself, as in the case of a deterministic signal spectrum at the output of an odd nonlinearity, and expressed by

$$\begin{aligned} S_{s_d s_d}(v) &= \mathrm{FT}\{R_{s_d s_d}(\tau)\} \\ &= \alpha^2 S_{ss}(v) + S_{n_d n_d}(v) \\ &= \frac{c_0}{(2\sigma^2)} S_{ss}(v) + \sum_{n=1}^{\infty} \frac{c_n}{(2\sigma^2)^{2n+1}} \\ &\quad \cdot [S_{ss}(v) \otimes_1 \cdots \otimes_{2n+1} S_{ss}(v)] \end{aligned} \tag{9}$$

where $\mathrm{FT}\{\cdot\}$ is the Fourier transform operator and v the frequency variable.

III. OFDM Performance in Nonlinear AWGN Channel

The uncoded system performance in AWGN channels is generally expressed by

$$\mathrm{SER} = P_{\mathrm{err}}(\mathrm{SNR}) \tag{10}$$

where SNR is the signal-to-noise ratio at the receiver input. The SNR is related to the E_b/N_0 ratio by the following expression:

$$\mathrm{SNR} = n_{\mathrm{bit}} \cdot \frac{E_b}{N_0} \tag{11}$$

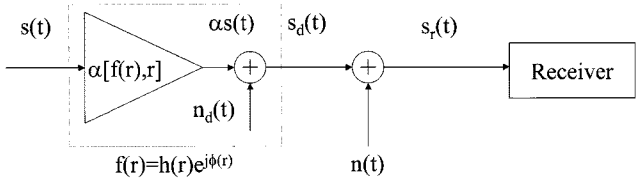

Fig. 2. Equivalent nonlinear AWGN channels for Gaussian signal.

where E_b is the energy per bit in a symbol period, N_o is the PSD of a white Gaussian noise and n_{bit} are the bits per symbol transmitted. The complex baseband samples of an OFDM signal transmitted during an OFDM symbol duration $T_b = L_{\text{fft}}T_s$ is expressed by (12) [13] where $z[k] = ak + jb_k$ represents the unmodulated complex information symbols, $\omega_k = k/T_b$ the angular frequency of the kth carrier, and L_{fft} the number of carriers.

$$\begin{aligned} s[m] &= s(mT_s) \\ &= \sum_{k=0}^{L_{\text{fft}}-1} z[k]e^{j\omega_k mT_s}, \qquad m = 0, \cdots, L_{\text{fft}} - 1. \end{aligned} \tag{12}$$

The symbols $z[k]$ transmitted over each carrier are mapped on a complex domain (M-QAM, M-DPSK, M-FSK) which is imposed by the application (DAB, DVB-T, WLAN, ADSL, etc).

The complex signal received through the nonlinear AWGN channel represented in Fig. 2 is expressed by

$$\begin{aligned} s_r(t) &= s_d(t) + n_r(t) \\ &= s_u(t) + n_d(t) + n_r(t) \\ &= \alpha \cdot s(t) + n_d(t) + n_r(t). \end{aligned} \tag{13}$$

The symbols received on the kth carrier are expressed, after the discrete Fourier transform (DFT) processing, by

$$\begin{aligned} z_r[k] &= \sum_{m=0}^{L_{\text{fft}}-1} s_r(m_s) \cdot e^{-j(2\pi/L_{\text{fft}})mk} \\ &= \alpha \cdot z[k] + \sum_{m=0}^{L_{\text{fft}}-1} [n_d(mT_s) + n_r(mT_s)] \cdot e^{-(2\pi/L_{\text{fft}})mk} \\ &= \alpha \cdot z[k] + e_{n_d}[k] + e_{n_r}[k] \\ &= \alpha \cdot z[k] + e_n[k]. \end{aligned} \tag{14}$$

The $\alpha z[k]$ term in (14) is the useful one (i.e., the undistorted data) when the phase of the α complex coefficient is opportunely compensated at the receiver. This common phase rotation introduced on the constellation of each carrier by the AM/PM curve (through the α coefficient) is not influent in DAB systems because they make use of a differential phase modulation like $\pi/4$ shifted-DQPSK. The $e_{n_d}[k]$ and $e_{n_r}[k]$ terms, obtained by DFT of the distortion noise contribution $n_d(mT_s)$ and of the AWGN contribution $n_r(mT_s)$, are two uncorrelated noise contributions that distort the received symbols. The $e_{n_d}[k]$ contribution is obtained by linear combination of samples of a stationary process. It can be modeled as a complex Gaussian process, because of the central limit theorem, if the number of the distortion errors that occurs in the time-domain during the T_b duration of each OFDM symbol is high enough. In this sense, the $e_{n_d}[k]$ distortion affects the constellation mapped over each carrier, in the same way as the Gaussian noise term $e_{n_r}[k]$ obtained by DFT of the thermal Gaussian noise of the receiver [14]. As a consequence, the system performance of an OFDM system can be derived, making use of the same relation used for AWGN channels with the attention of redefining the effective SNR at the receiver input taking into account the nonlinear distortion noise contribution. The nonlinear distortion noise is uncorrelated with the thermal noise; they can be added in power to estimate the BER performance by (10).

$$\begin{aligned} P_{e_n}[k] &= E\{e_n[k] \cdot e_n^*[k]\} \\ &= L_{\text{act}} \cdot S_{nn}\left(\frac{k}{T_b}\right) \\ &= L_{\text{act}} \cdot S_{n_d n_d}\left(\frac{k}{T_b}\right) + L_{\text{act}} \cdot S_{n_r n_r}\left(\frac{k}{T_b}\right). \end{aligned} \tag{15}$$

It is easy to show (see Appendix IV), by means of (14) that the noise power term $P_{e_n}[k]$ and the useful power term $P_{z_u}[k]$ are expressed, for each carrier, by (15) and (16).

$$P_{z_u}[k] = |\alpha|^2 \cdot E\{z[k] \cdot z^*[k]\} = |\alpha|^2 \cdot L_{\text{act}} \cdot S_{ss}\left(\frac{k}{T_b}\right) \tag{16}$$

where $S_{n_d n_d}(v)$, $S_{n_r n_r}(v)$, and $S_{ss}(v)$ represent the PSD of the corresponding signals, L_{act} represents the number of the switched-on carriers within the total, L_{fft} carriers and $(L_{\text{fft}} - L_{\text{act}})$ are the switched-off carriers which represent the guard band of the OFDM system. The two powers expressed by (15) and (16), respectively, represent the sampling on the kth carrier position of the PSD of the noise terms $n_r(t)$ and $n_d(t)$ and of the useful term $s(t)$ in (13).

From the above consideration, it should be clear that the BER performance of the kth subchannel associated to the kth carrier of the OFDM signal depends both on the nonlinear distortion noise and on the thermal noise. The SNR at the receiver for the kth carrier, after the FFT processing, is generally defined as the power ratio between the received signal $z[k]$ and the thermal noise $n_r[k]$. This SNR will be named "apparent" in the following because it is not the only one that influences the performance. It is, however, the measurable one at the receiver and consequently the one in respect of which the BER is generally sketched and the one that is imposed in the simulations.

$(\text{SNR})_{\text{eff}}$ is the effective SNR that establishes the performance at the receiver in presence of nonlinear distortions, and it is defined as the power ratio between the useful signal $z_u[k]$ and the total noise $e_n[k]$, after the FFT processing. $(\text{SNR})_{nl}$ is the power ratio at the receiver in absence of the thermal noise, and it is defined as the power ratio between the useful signal $z_u[k]$ and the nonlinear noise $e_{nl}[k]$. The above quantities are expressed in the (17)–(19) for the generic kth carrier of the OFDM system.

$$\begin{aligned} [(\text{SNR})_{nl}]_k &= \frac{P_{z_u}[k]}{P_{e_{nl}}[k]} \\ &= \frac{|\alpha|^2 \cdot P_z[k]}{P_{e_{nl}}[k]} \\ &= \frac{c_0^2}{2\sigma^2} \frac{S_{ss} \cdot \left(\frac{k}{T_b}\right)}{S_{n_d n_d}\left(\frac{k}{T_b}\right)} \end{aligned} \tag{17}$$

$$
\begin{aligned}
[(\mathrm{SNR})_{\mathrm{app}}]_k &= \frac{P_{Z_d}[k]}{P_{e_{nr}}[k]} \\
&= \frac{P_{Z_u}[k] + P_{e_{nd}}[k]}{P_{e_{nr}}[k]} \\
&= \frac{S_{s_d s_d}\left(\dfrac{k}{T_b}\right)}{N_0} \\
&= \frac{|\alpha|^2 S_{ss}\left(\dfrac{k}{T_b}\right) + S_{n_d n_d}\left(\dfrac{k}{T_b}\right)}{N_0}
\end{aligned} \tag{18}
$$

$$
\begin{aligned}
[(\mathrm{SNR})_{\mathrm{eff}}]_k &= \frac{P_{z_u}[k]}{P_{e_{nr}}[k] + P_{e_{nd}}[k]} \\
&= \frac{P_{z_u}[k]}{\dfrac{P_{z_u}[k] + P_{e_{nd}}[k]}{(\mathrm{SNR})_{\mathrm{app}}} + P_{e_{nd}}[k]} \\
&= \left\{[(\mathrm{SNR})_{\mathrm{app}}]_k^{-1} + [1 + [(\mathrm{SNR})_{\mathrm{app}}]_k^{-1}] \right. \\
&\quad \left. \cdot [(\mathrm{SNR})_{nl}]_k^{-1}\right\}^{-1}.
\end{aligned} \tag{19}
$$

P_x and S_{xx} are used to indicate respectively the power and the PSD of the 'x' signal. The calculation of the above quantity depends on the $f(r)$ nonlinearity by (6) and (7).

The uncoded error probability of (10) can be derived for a DAB system bearing in mind that the symbol-error rate (SER) for a single-carrier $\pi/4$ Sshifted-DQPSK mapping in the AWGN channel is expressed by [21]

$$
\begin{aligned}
\mathrm{SER} &= Q_m^{(1)}(a,b) - 0.5 \cdot I_0(a \cdot b) \cdot e^{-0.5\cdot(a^2+b^2)} \\
Q_m^{(10}(a,b) &= e - 0.5 \cdot (a^2 + b^2) + \sum_{k=0}^{\infty} \left(\frac{a}{b}\right)^k I_k(ab) \\
a &= \sqrt{(1 - \sqrt{0.5} \cdot \mathrm{SNR}} \\
b &= \sqrt{(1 + \sqrt{0.5}) \cdot \mathrm{SNR}}
\end{aligned} \tag{20}
$$

where $Q_m^{(1)}(a,b)$ is the first-order Marcum function and $I_k(x)$ is the kth-order modified Bessel function. In multicarrier systems like DAB, the mean BER for all the carriers is obtained by

$$
\mathrm{BER} = \frac{\mathrm{SER}}{n_{\mathrm{bit}}} = \frac{1}{2 \cdot L_{\mathrm{data}}} \sum_{k=1}^{L_{\mathrm{data}}} (\mathrm{SER})_k \tag{21}
$$

which represents the average of the BER values calculated on L_{data}, the carriers (with $L_{\mathrm{data}} < L_{\mathrm{act}} < L_{\mathrm{fft}}$)) which are used to transmit data. The values of $(\mathrm{SER})_k$ for each carrier, in presence of nonlinear distortions, is calculated by (20), making use of (19) to express the effective SNR that establishes the system performance.

IV. Nonlinear Amplifiers and Ideal Predistortion

In this section, we are interested in obtaining an easily manageable expression for the c_n coefficients of (7) when $f(r)$ represents the nonlinear distortion introduced by an instantaneous power amplifier with and without ideal predistortion. The Bessel series expansion is a typical representation [15]–[18] of the $f(r)$ function for the power amplifier that introduces nonlinear distortions, as expressed in (22) or (B.1)

$$
\begin{aligned}
f(r) &= h(r) e^{j\phi(r)} \\
&= \sum_{m=0}^{L} b_m J_1\left(\frac{(2m-1)\pi}{R_{\max}} \cdot r\right) \\
&= \sum_{m=0}^{L} b_m J_1\left(\beta(m,\gamma)\frac{\sqrt{\gamma}}{A} r\right)
\end{aligned} \tag{22}
$$

with $h(r)$ and $\phi(r)$, respectively, the AM/AM and the AM/PM distortion curves. The b_m coefficients can be derived by fitting procedures on the measured data [16]. The γ term in (22) is the input-backoff and represents the ratio between the input saturation power and the input mean power as expressed by (23), where A is the input amplitude of the maximum amplifier output power and $2\sigma^2$ is the signal input power.

$$
\gamma = \frac{A^2}{2\sigma^2}. \tag{23}
$$

The c_n coefficients are obtained by substituting (22) in (7) and are expressed by (24).

$$
\begin{aligned}
c_n &= \frac{1}{n!(n+1)!} \\
&\quad \cdot \left\| \sum_{m=0}^{L} b_m \cdot \left[\frac{\beta(m,\gamma)}{2}\right]^{2n+1} \cdot e^{-[\beta(m,\gamma)/2]^2} \right\|^2.
\end{aligned} \tag{24}
$$

The c_n coefficients depend on the $f(r)$ nonlinearity, through the b_m coefficients of the Bessel expansion (22), and on the γ input-backoff, through the $\beta(m,\gamma)$ coefficients (see Appendix II). The Bessel series expansion of the complex nonlinear characteristic of a power amplifier allows to correctly represent almost any kind of amplifier, by using an appropriate number of b_m coefficients to make the fitting error as low as possible. The Saleh model [19] is another typical representation of the complex nonlinear function of a power amplifier. This model has gained a lot of popularity because it represents the complex nonlinear function by an easier analytical notation as expressed by (25)

$$
h(r) = \frac{\alpha_h r}{1 = \beta_h r^2}, \qquad \phi(r) = \frac{\alpha_\phi r^2}{1 + \beta_\phi r^2} \tag{25}
$$

or equivalently

$$
f(r) = h(r) e^{j\phi(r)} = \frac{\alpha_r r}{1 + \beta_r r^2} + j\frac{\alpha_i r}{1 + \beta_i r^2} \tag{26}
$$

where only four coefficients are needed to fit the complex nonlinear function of the amplifier by minimizing the root-mean-square error. Compared to the Bessel series expansion, the Saleh model can be applied to a narrower class of amplifiers, characterized by regular shapes of the AM/AM and AM/PM curves like the ones of typical TWT's (traveling waves tubes). Nevertheless, the approach presented in this paper does not depend on the amplifier model. As a consequence, if the Saleh model is used to represent the amplifier, the c_n coefficients can be derived by substituting (25) or (26) in (7). Unfortunately, an analytical solution of such integral is not available at this moment, and consequently it must be numerically evaluated.

Otherwise, $f(r)$ is reduced to a real function expressed by (27) if the RF amplifier is ideally predistorted

$$f(r) = h(r) = \begin{cases} r, & r \le A \\ A, & r > A. \end{cases} \tag{27}$$

In fact, the AM/PM can be completely cancelled by an ideal predistorter, while the AM/AM can only be inverted as far as the saturation power. In this case, the ideally predistorted amplifier exhibits a residual AM/AM that acts as a soft-limiter on the input envelope [16]. In this situation, it is possible to express the c_n coefficients by means of an exact expression, through the following relations [(28)] (see Appendix III) where $\operatorname{erfc}(x)$ is the complementary error function, that is $\operatorname{erfc}(x) \equiv 1 - (2/\sqrt{\pi}) \int_0^x e^{-t^2}\, dt$.

$$\begin{aligned} c_0 &= 2\sigma^2 \cdot \left[1 - e^{-\gamma} + \frac{1}{2}\sqrt{\pi \cdot \gamma} \cdot \operatorname{erfc}(\sqrt{\gamma})\right]^2 \\ c_1 &= \frac{1}{2}\left[\frac{1}{2}\gamma \cdot e^{-\gamma} + \frac{1}{4}\sqrt{\pi \cdot \gamma} \cdot \operatorname{erfc}(\sqrt{\gamma})\right]^2 \\ c_n &= \frac{1}{n!(n+1)!}\left[\left(\frac{(2n)!}{2^{2n} n!} - \sum_{i=0}^{n-2} d_{i,n}\gamma^{i+1}\right)\gamma e^{-\gamma} \right. \\ &\quad \left. + \frac{(2n)!}{2^{2n+1} n!}\sqrt{\pi\gamma}\operatorname{erfc}(\sqrt{\gamma})\right]^2, \qquad n = 2, \cdots, \infty. \end{aligned} \tag{28}$$

The coefficients in (28) are recursively obtained by (29) (see Appendix III)

$$\begin{cases} p_{0,n} = \dfrac{(n+1)!}{2}, & i = 0 \\ p_{i,n} = p_{i-1,n-1} + (n+1)p_{i,n-1}, & i = 1, \cdots, n-2 \end{cases}$$

$$\begin{cases} q_{0,n} = \dfrac{1}{3}\left[\dfrac{(n+1)!}{2} - \dfrac{(2n)!}{2^{2n-1} \cdot n!}\right], & i = 0 \\ q_{i,n} = \dfrac{1}{3}(p_{i,n} - 2q_{i-1,n}), & i = 1, \cdots, n-2 \end{cases}$$

$$d_{i,n} = \frac{1}{i!}\sum_{p=}^{n-2} q_{p,n}\left[\sum_{m=1}^{i} (-1)^m \binom{i}{m} m^p\right], \quad i = 0, \cdots, n-2. \tag{29}$$

The first values of the $d_{i,n}$ coefficient in (29) are outlined in Table I.

TABLE I
FIRST VALUES OF THE RECURSIVE COEFFICIENTS

$d_{i,n}$	$i=0$	$i=1$	$i=2$
$n=2$	$-\frac{1}{2}$	0	0
$n=3$	$-\frac{11}{4}$	$\frac{1}{2}$	0
$n=4$	$-\frac{125}{8}$	$\frac{23}{4}$	$-\frac{1}{2}$

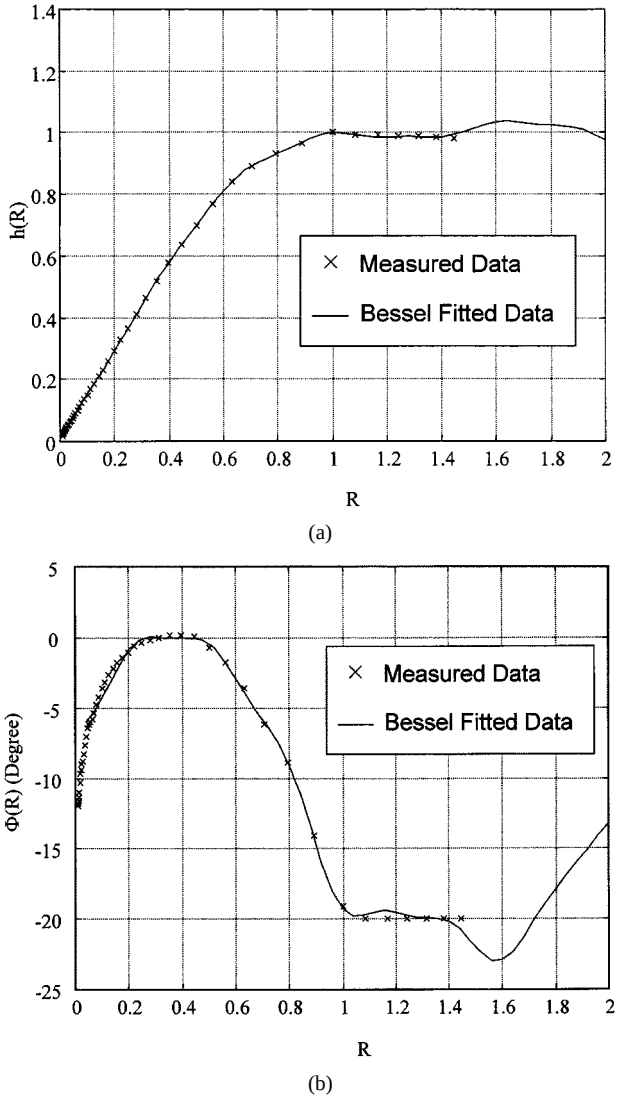

Fig. 3. Measured (a) AM/AM and (b) AM/PM representation by Bessel series expansion.

V. SIMULATION RESULTS

The performance comparison between analytical results and computer simulation is demonstrated in this section, as a confirmation of the analytical approach. The DAB system has been chosen as a reference, but the conclusions are extensible to any OFDM system as long as the L_{fft} size is large enough to satisfy the Gaussian signal assumption. The DAB, as with most OFDM systems, uses a cyclic extension of the inverse fast Fourier transform output in order to compensate for multipath at the receiver. This aspect is not considered in our analysis estimating the OFDM PSD because it does not impact on the system performance in nonlinear AWGN channels. In the simulation approach, the PSD was estimated, by means of periodogram, as the average of the PSD (calculated by DFT) of each interpolated (by four) OFDM block. As a consequence, each OFDM block shows a quasi-rectangular PSD without significant power contribution in the guard-band region. The PSD obtained in this way is not comparable with the one measured by a spectrum analyzer in a real system, because it does not take into account the phase discontinuities between adjacent OFDM blocks, which cause the spread of the PSD in the adjacent guard-bands. Moreover, the PSD measured by a spectrum analyzer strongly depends on the used video bandwidth, resolution bandwidth, and video averaging. However, it is possible to compare the real measurement with analytical results obtained by the proposed approach, by substituting the PSD measured in linear conditions

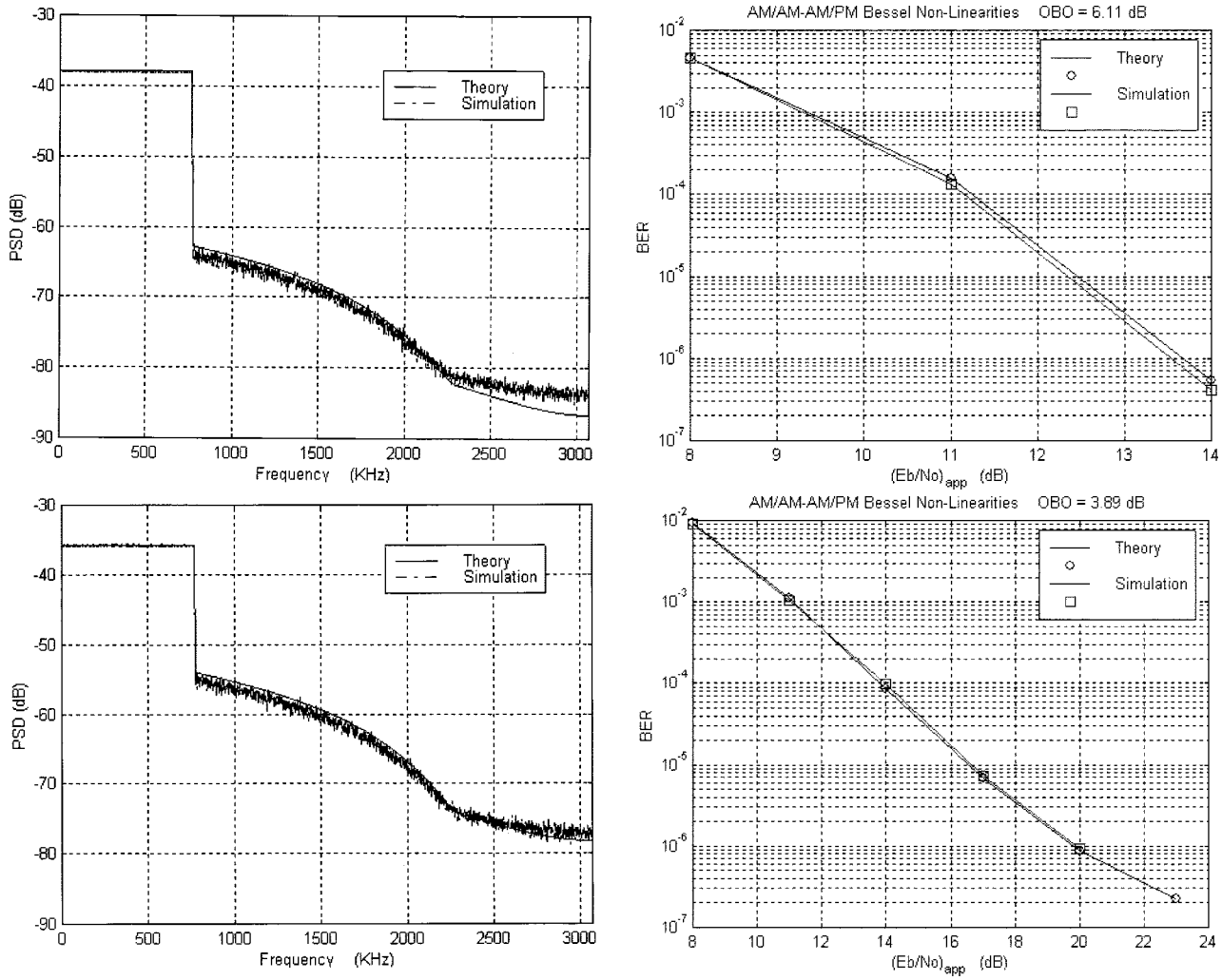

Fig. 4. DAB performance with AM/AM–AM/PM nonlinearities.

at the right-hand side of (9) or, equivalently, substituting its inverse Fourier transform into (6).

The DAB signal in the Mode I operating condition ($L_{\text{fft}} = 2048$) [2] is formed by 2048–length blocks characterized by 1 msec of duration (without the cyclic prefix), whose values have been oversampled four times in order to obtain an adequate signal representation in a nonlinear environment. The signal envelope of each interpolated block has been distorted during simulation by the curves (27) and (22) that represent the AM/AM–AM/PM distorting amplifier with and without ideal predistortion, respectively.

Both the BER degradation and the spectral regrowth have been evaluated for different γ (input-backoff). Eighty OFDM blocks have been used to estimate the PSD by simulation, in the way previously explained. Fig. 3 shows the AM/AM and AM/PM curves fitted by (22) using ten b_m coefficients while the corresponding obtained results are shown in Fig. 4. Both the PSD regrowth and the corresponding uncoded BER degradation are outlined by using (9) and (21), respectively.

Fig. 5 shows the same results when we take into account the ideal predistortion condition expressed by (27). All the analytical expressions used to obtain the system performance depend on the input-backoff (γ) value. However, it is important to estimate the output-backoff (obo) for a meaningful comparison of the predistorted and nonpredistorted conditions. The obo is defined as the ratio between the maximum and the mean output power. It generally depends on both the γ value and on the $f(r)$ nonlinear distortion, as expressed by

$$obo = \frac{P_{\text{out,Max}}}{\overline{P}_{\text{out}}} = F[\gamma, f(r)]. \tag{30}$$

In the ideal predistortion case, the above expression becomes [20]

$$\text{obo} = \gamma \cdot (1 - e^{-\gamma}). \tag{31}$$

A performance comparison between the predistorted and nonpredistorted conditions is beyond the scope of this paper, as well as considerations about the optimum criterion to fix the *obo* in an OFDM system, and it will be the subject of future works.

However, an optimum agreement between simulated and analytical results is outlined by Figs. 4 and 5 both for the nonpredistorted and ideally predistorted amplifier when the obo is not too high (i.e., $obo < (9/10)$ dB). For higher obo values, the estimated PSD upper-bounds the simulated one. This fact can be explained because OFDM signals are not exactly Gaussian distributed, and their envelope is not perfectly Rayleigh distributed.

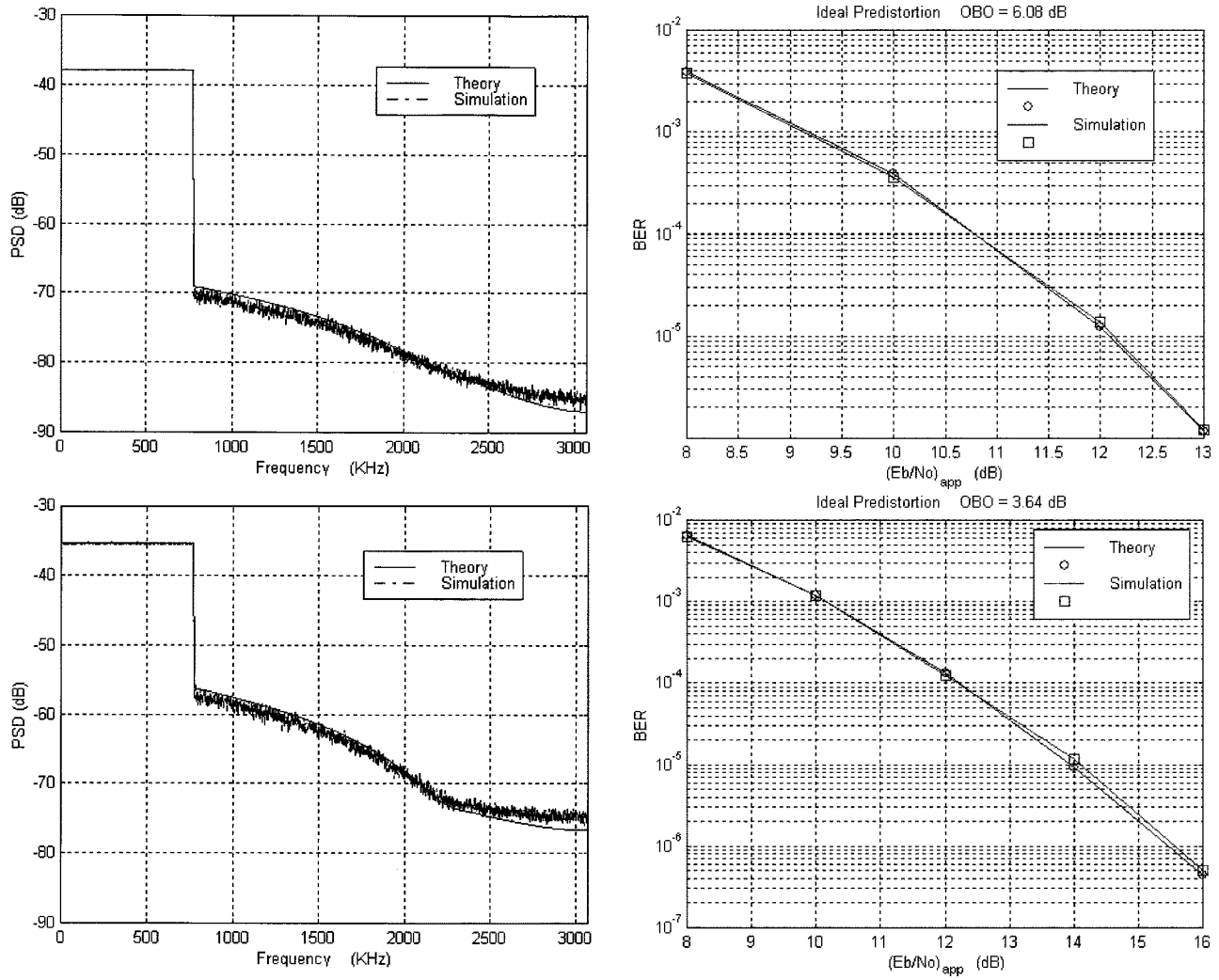

Fig. 5. DAB performance with ideal predistortion.

In particular, the maximum envelope will never be infinite, and the accuracy of approximating the pdf with a Rayleigh function is lower for high envelope values. For a certain nonlinear distortion $f(r)$, the increase of the γ value means the reduction of the σ standard deviation of the Gaussian input [see (23)], and as a consequence, the input signal is compressed in the lower region of the $f(r)$ curve.

Power amplifiers are usually characterized (especially Class A amplifiers) by $f(r)$ curves that are quasi-linear for low input values and that localize the distortions in the higher power zone. As a consequence, for high γ values, the nonlinear distortions occur prevalently in correspondence of input envelopes that belong to the right end part of the OFDM pdf where the Rayleigh approximation does not hold anymore. This implies that the c_n coefficient evaluation by (7) is not exact and the resulting PSD does not agree with the simulated one when the γ value is too high. The approximation error is reduced if the L_{fft} carrier number becomes higher, and consequently, the OFDM signal is better approximated by a Gaussian pdf. An ideally predistorted amplifier distorts the signal only for the high input powers after the saturation zone and, as a consequence, is more sensitive to the inadequate analytical representation for high input-backoff. For practical γ values below 9 dB, however, the PSD results testify to the correctness of the analytical derivation of the c_n coefficients for the output correlation function (6), while the BER results testify to the correctness of the proposed model for nonlinear AWGN channels.

Similar considerations can moreover be extended to nonlinear fading channels when the equalization technique at the receiver is considered [16]. Finally, Fig. 6 shows the baseband output PSD for a 2000–carrier OFDM system in linearized environment. Each term's contribution of (6) to the signal spectral re-growth is outlined for two different obo values.

VI. Conclusions

We have reviewed the analytical background for expressing the output correlation function for complex Gaussian signals distorted by envelope dependent nonlinearities. Original results for AM/AM and AM/PM nonlinearities represented by Bessel series expansion have been derived. Original results are also outlined for the envelope clipping phenomenon which may be compared with the known results for the cartesian clipping [10], [23]–[25]. The envelope clipping is particularly interesting because it represents the ideal predistortion of the AM/AM and AM/PM nonlinearities introduced by high power amplifiers.

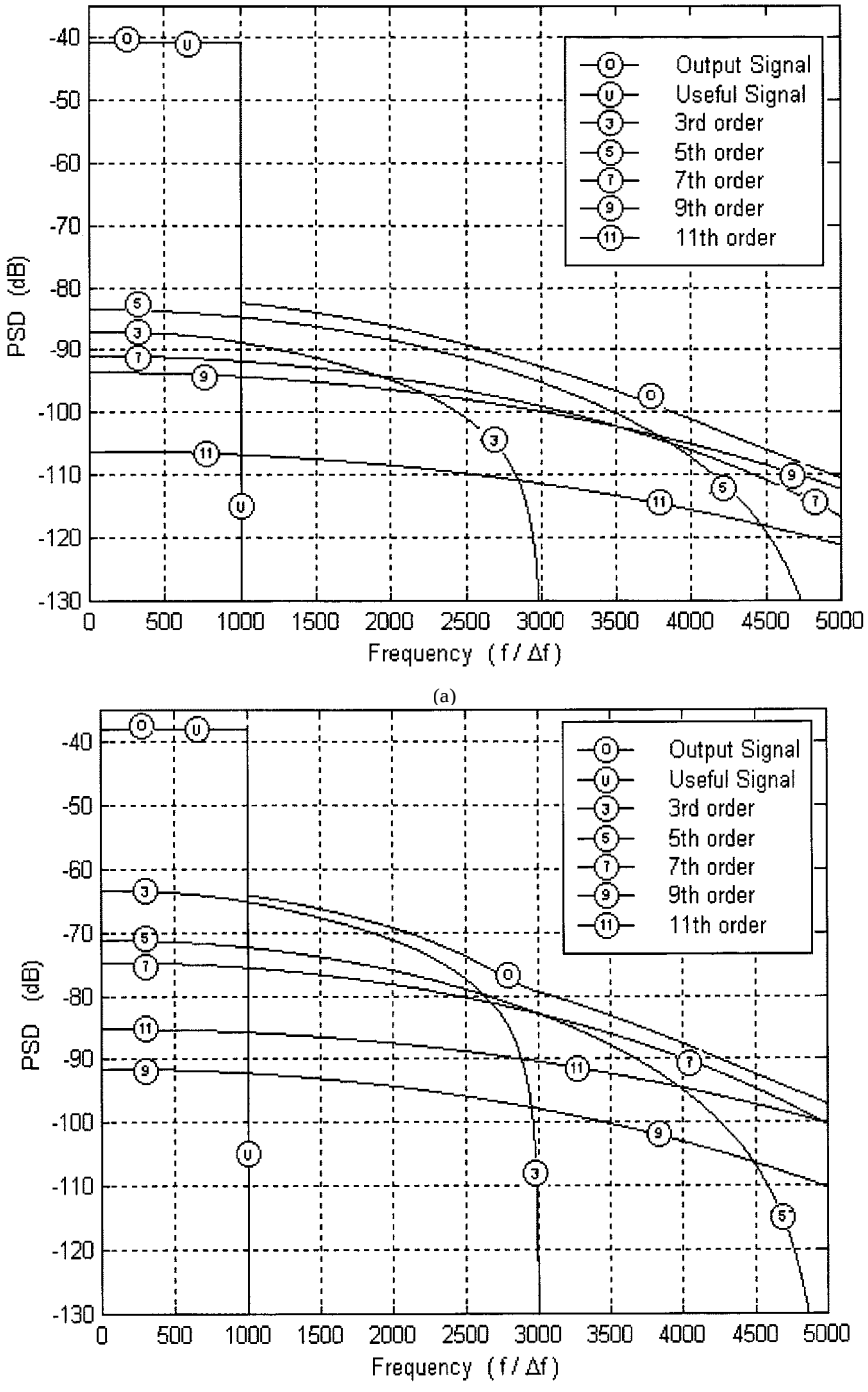

Fig. 6. Spectral components of an envelope clipped OFDM signal. (a) Ideal predistortion: N° carriers = 2000; $\gamma = 6$ dB; obo = 6.08 dB. (b) Ideal predistortion: N° carriers = 2000; $\gamma = 3$ dB; obo = 3.63 dB.

These results have been used to propose a model for the analytical performance evaluation of OFDM systems in nonlinear AWGN channels. Computer simulations have validated both the proposed model and the analytical derivations. This approach constitutes a generalization and an improvement of the semianalytical approach already known in the literature [14]. The computer calculation time to predict the OFDM system performance has been dramatically reduced. The proposed approach can also be extended to nonlinear fading channels, in order to outline the OFDM system performance in realistic environments. In this case, the effects of the nonlinear distortion noise on the equalizer performance must be taken into account, and this will be the subject of future work.

Appendix A
Output Correlation Function for Nonlinear Distortions that Depend on Complex Gaussian Signal Envelope

Denote

$$s(t) = x(t) + jy(t) = r(t) \cdot \exp[j\theta(t)] \qquad \text{(A.1)}$$

a complex stationary Gaussian process with equal distributed, zero-mean, independent $x(t)$ and $y(t)$ components. Under these defined hypotheses

$$\begin{aligned} x_1 &= x(t), \qquad x_2 = x(t+\tau) \\ y_1 &= y(t), \qquad y_2 = y(t+\tau) \end{aligned} \tag{A.2}$$

the joint pdf is expressed by

$$\begin{aligned} &p(x_1, x_2, y_1, y_2) \\ &\quad = p(x_1, x_2) \cdot p(y_1, y_2) \\ &\quad = \frac{1}{(2\pi)^2 \sigma^4 (1-\rho^2)} \\ &\qquad \cdot \exp\left(-\frac{(x_1^2+y_1^2)+(x_2^2+y_2^2)-2\rho(x_1x_2+y_1y_2)}{2\sigma^2(1-\rho^2)} \right) \end{aligned} \tag{A.3}$$

with the autocorrelation coefficient ρ and the input power $2\sigma^2$, respectively, expressed by

$$\begin{aligned} \rho &= \frac{R_{xx}(\tau)}{\sigma^2} \\ &= \frac{E\{x_1 x_2\}}{E\{x_1^2\}} \\ 2\sigma^2 &= R_{ss}(0) \\ &= 2R_{xx}(0) \end{aligned} \tag{A.4}$$

with $E\{xy\}$ the statistical expectation

$$E\{xy\} = \iint xy \cdot p(x,y)\, dx\, dy. \tag{A.5}$$

The input correlation function is by definition expressed by

$$\begin{aligned} R_{ss}(\tau) &= E\{s^*(t)s(t+\tau)\} \\ &= E\{s_1^* s_2\} \\ &= E\{(x_1 - jy_1)(x_2 + jy_2)\} \\ &= [R_{xx}(\tau)+R_{yy}(\tau)]+j[R_{xy}(\tau)-R_{yx}(\tau)]. \end{aligned} \tag{A.6}$$

The above expression, for a complex process $s(t)$ with equally distributed and independent real components, becomes

$$R_{ss}(\tau) = 2 \cdot R_{xx}(\tau). \tag{A.7}$$

If $f(r)$ represents the complex nonlinear distortion function, which only depends on the input envelope of $s(t)$, then the output distorted signal is expressed by

$$s_d(t) = g[s(t)] = g\lfloor r(t)e^{j\theta(t)} \rfloor = f[r(t)] \cdot e^{j\theta(t)}. \tag{A.8}$$

Based on the above definitions, the output correlation function is given by

$$\begin{aligned} R_{s_d s_d} &= E\{s_d^*(t) s_d(t+\tau)\} \\ &= E\{g^*(r_1 e^{j\theta_1}) g(r_2 e^{j\theta_2})\} \\ &= \iiiint\limits_{D(x_1,x_2,y_1,y_2)} g^*(x_1,y_1) g(x_2,y_2) \\ &\qquad \cdot p\,(x_1,x_2,y_1,y_2)\, dx_1\, dy_1\, dx_2\, dy_2. \end{aligned} \tag{A.9}$$

The integral in (A.9) in polar coordinates becomes

$$\begin{aligned} R_{zz}(\tau) = &- \iiiint\limits_{D(r_1,r_2,\theta_1,\theta_2)} g^*(r_1 e^{j\theta_1}) g(r_2 e^{j\theta_2}) \\ &\cdot p(r_1 \cos\theta_1, r_2 \cos\theta_2) \\ &\cdot p(r_1 \sin\theta_1, r_2 \sin\theta_2) \cdot r_1 r_2\, dr_1\, dr_2\, d\theta_1\, d\theta_2. \end{aligned} \tag{A.10}$$

With some manipulations, substituting (A.8) and (A.3) into (A.10), it is straightforward to obtain

$$\begin{aligned} R_{zz}(\tau) = &\frac{2}{\alpha(2\pi\sigma)^2} \iint\limits_{D(r_1,r_2)} f^*(r_1) f(r_2) r_1 e^{-(r_1/\alpha)} r_2 e^{-(r_2/\alpha)} \\ &\cdot \left(\int_0^{2\pi}\int_0^{2\pi} \cos(\theta_1 - \theta_2) \right. \\ &\left. \cdot\, e^{(-2\rho r_1 r_2/\alpha)\cos(\theta_1-\theta_2)}\, d\theta_1\, d\theta_2 \right) dr_1\, dr_2 \end{aligned} \tag{A.11}$$

with $\alpha = 2\sigma^2(1-\rho^2)$.

The double integral in (A.11) is computable by modified Bessel functions to obtain

$$\begin{aligned} R_{zz}(\tau) = &\iint\limits_{D(r_1,r_2)} f^*(r_1) f(r_2) \cdot \frac{r_1 r_2}{\sigma^4(1-\rho^2)} e^{-(r_1^2+r_2^2)/2\sigma^2(1-\rho^2)} \\ &\cdot I_1\left[\frac{\rho r_1 r_2}{\sigma^2(1-\rho^2)} \right] dr_1\, dr_2 \end{aligned} \tag{A.12}$$

where $I_1(\cdot)$ is the modified Bessel function of the first order and first kind.

Making use of the Laguerre polynomial series expansion [22, eq. (5.11.3.7)], expressed by (A.13)

$$\begin{aligned} &\sum_{n=0}^{\infty} \frac{1}{n+1} \cdot \rho^{2n} \cdot L_n^{(1)}\left(\frac{r_1^2}{2\sigma^2}\right) \cdot L_n^{(1)}\left(\frac{r_2^2}{2\sigma^2}\right) \\ &\qquad = \frac{e^{-\rho^2(r_1^2+r_2^2)/(1-\rho^2)2\sigma^2}}{(1-\rho^2)\cdot\rho\dfrac{r_1 r_2}{2\sigma^2}} \cdot I_1\left[\frac{\rho r_1 r_2}{\sigma^2(1-\rho^2)}\right] \end{aligned} \tag{A.13}$$

and substituting it into (A.12), the expression of the output correlation function becomes (A.14).

$$\begin{aligned} R_{zz}(\tau) = &\frac{1}{2\sigma^2} \iint\limits_{D(r_1 r_2)} f^*(r_1) f(r_2) \cdot \frac{r_1^2}{\sigma^2}\,\frac{r_2^2}{\sigma^2} \cdot e^{-(r_1^2+r_2^2)/2\sigma^2} \\ &\cdot \left[\sum_{n=0}^{\infty} \frac{\rho^{2n+1}}{n+1} \cdot L_n^{(1)}\left(\frac{r_1^2}{2\sigma^2}\right) \cdot L_n^{(1)}\left(\frac{r_2^2}{2\sigma^2}\right) \right] dr_1\, dr_2. \end{aligned} \tag{A.14}$$

The double integral in (A.14) is separable in respect to r_1 and r_2 to obtain the general expression (A.15).

$$\begin{aligned} R_{zz}(\tau) = &\frac{1}{2\sigma^2} \sum_{n=0}^{\infty} \frac{1}{n+1} \\ &\cdot \left| \int_{D(r)} f(r) \frac{r^2}{\sigma^2} e^{-r^2/2\sigma^2} L_n^{(1)}\left(\frac{r^2}{2\sigma^2}\right) dr \right|^2 \rho^{2n+1}. \end{aligned} \tag{A.15}$$

Appendix B
Nonlinear Amplifier with AM/AM and AM/PM Expressed by Bessel Series Expansion

If $f(r)$ is the complex AM/AM and AM/PM distortion function, it can be represented by Bessel series expansion (B.1) where b_m are $(L+1)$ complex coefficients

$$f(r) = h(r)e^{j\phi(r)} = \sum_{m=0}^{L} b_m J_1\left(\beta \frac{r}{\sqrt{2}\cdot\sigma}\right). \tag{B.1}$$

The β parameter may be chosen equal to (B.2) to be compliant with the notation used in [16], with $2\sigma^2$ representing the input power, $R_{\max}$ a normalization factor, A the input amplitude to which corresponds the saturation power, and γ the input-backoff defined in (23).

$$\beta = \beta(m,\gamma) = \frac{(2m-1)\pi}{R_{\max}}\sqrt{2}\cdot\sigma = \frac{(2m-1)\pi}{R_{\max}}\cdot\frac{A}{\sqrt{\gamma}}. \quad \text{(B.2)}$$

Substituting (B.1) into (10), we obtain the following expression for the coefficients:

$$\begin{aligned} c_n &= \frac{1}{2\sigma^2}\,\frac{1}{n+1}\cdot\left\|\int_{D(r)}\sum_{m=0}^{L} b_m J_1\left(\beta(m,\gamma)\frac{r}{\sqrt{2}\cdot\sigma}\right)\right. \\ &\qquad \left.\cdot\,\frac{r^2}{\sigma^2}e^{-r^2/2\sigma^2}L_n^{(1)}\left(\frac{r^2}{2\sigma^2}\right)\,dr\right\|^2 \\ &= \frac{1}{n+1}\cdot\left\|\sum_{m=0}^{L} b_m\int_0^{\infty}\sqrt{y}\cdot e^{-y}J_1[\beta(m,\gamma)\cdot\sqrt{y}]\right. \\ &\qquad \left.\cdot\,L_n^{(1)}(y)\,dy\right\|^2. \end{aligned} \quad \text{(B.3)}$$

The above integral is analytically solvable [22, eq. (2.19.12.6)] and (B.3) becomes

$$c_n = \frac{1}{n!(n+1)!}\cdot\left\|\sum_{m=0}^{L} b_m\cdot\left(\frac{\beta(m,\gamma)}{2}\right)^{2n+1}\cdot e^{-(\beta(m,\gamma)/2)^2}\right\|^2 \quad \text{(B.4)}$$

which coincides with (24). It should be highlighted that the Bessel series representation (B.1) of the amplifier nonlinearity does not depend on the signal input power $2\sigma^2$ (i.e., on the γ input-backoff). The PSD on the contrary depends on the γ input-backoff trough, the β parameter of (B.2).

Appendix C
Ideal Predistortion (Envelope Soft-Limiter)

In this case, the nonlinear function $f(r)$ is a real function expressed by

$$f(r) = h(r) = \begin{cases} r, & r \le A \\ A, & r > A. \end{cases} \quad \text{(C.1)}$$

Substituting (C.1) into (10), the expression of the c_n coefficients becomes (C.2) with a variable change expressed by $y = r^2/\sigma^2$.

$$\begin{aligned} c_n = \frac{1}{n_1}\cdot\left\{\int_0^{A/2\sigma^2} y\cdot e^{-y}\cdot L_n^{(1)}(y) + \frac{A}{\sqrt{2}\sigma}\right. \\ \cdot\left[\int_0^{\infty}\sqrt{y}\cdot e^{-y}\cdot L_n^{(1)}(y)\,dy\right. \\ \left.\left.-\int_0^{A/2\sigma^2}\sqrt{y}\cdot e^{-y}\cdot L_n^{(1)}(y)\,dy\right]\right\}^2. \end{aligned} \quad \text{(C.2)}$$

The integrals in (C.2) are all analytically solvable (the first and third by [22, eqs. (2.19.1.1), (2.19.3.5)], respectively), and after some manipulations it is possible to obtain

$$\begin{aligned} c_n = \frac{1}{n!(n+1)!}\left[\frac{(2n)!}{n!}\,\frac{\sqrt{\pi\cdot\gamma}}{2^{n+1}}\right. \\ \left.+\sum_{k=0}^{\infty}\frac{(n+k+1)!}{k!(k+1)!}\,\frac{(-1)^{k+1}}{(2k+3)}\cdot\gamma^{k+2}\right]^2 \end{aligned} \quad \text{(C.3)}$$

where $\gamma = A^2/2\sigma^2$ is the input-backoff in respect to the soft-limiter saturation point.

Expression (C.3) may be enough to calculate easily the c_n coefficient, if attention is paid to truncating the series expansions at a k-term high enough to make the error small enough. Anyway, it is possible to analytically calculate the sum of the series contained in (C.3) obtaining an exact closed-form expression for the c_n coefficients.

If $P_n(k)$ is the $(n-1)$th-order polynomial expressed by

$$\begin{aligned} P_n(k) &= \frac{(n+k+1)!}{(k+2)!} = (k+3)\cdot(k+4)\cdot\cdots\cdot(k+n+1) \\ &= p_{0,n} + p_{1,n}\cdot k + \cdots + p_{n-1,n}\cdot k^{n-1}. \end{aligned} \quad \text{(C.4)}$$

$Q_n(k)$ and $R_{0,n}$ are the quotient and the remainder of the division of $P_n(k)$ by $(2k+3)$, respectively, as expressed by

$$\begin{aligned} P_n(k) &= (2k+3)\cdot Q_n(k) + R_{0,n} \\ &= (2k+3)\cdot(q_{0,n} + q_{1,n}\cdot k \\ &\quad + \cdots + q_{n-2,n}\cdot k^{n-2} + R_{0,n} \\ &= (2k+3)\cdot\left(\sum_{i=0}^{n-2} q_{i,m}\cdot k^i\right) + R_{0,n}. \end{aligned} \quad \text{(C.5)}$$

The above expression is meaningful only for $n > 1$. Substituting (C.5) into (C.3), the c_n expression becomes

$$\begin{aligned} c_n &= \frac{1}{n!\cdot(n+1)!}\left[\frac{(2n)!}{n!}\,\frac{\sqrt{\pi\cdot\gamma}}{2^{n+1}}\right. \\ &\quad \left.+\sum_{k=0}^{\infty}\frac{(-1)^{k+1}}{k!}\,\frac{[(2k+3)\cdot Q_n(k)+R_{0,n}]}{(2k+3)}\cdot\gamma^{k+2}\right] \\ &= \frac{1}{n!\cdot(n+1)!}\left[\frac{(2n)!}{n!}\,\frac{\sqrt{\pi\cdot\gamma}}{2^{n+1}}\right. \\ &\quad +\sum_{i=0}^{n-2} q_{i,n}\sum_{k=0}^{\infty}\frac{(-1)^{k+1}}{k!}k^i\gamma^{k+2} + \frac{R_{0,n}}{2}\gamma \\ &\quad \left.\cdot\sum_{k=1}^{\infty}\frac{(-1)^k}{k!}\gamma^k - \frac{r_{0,n}}{2}\sqrt{\gamma}\cdot\sum_{k=1}^{\infty}\frac{(-1)^k}{k!}\,\frac{(\sqrt{\gamma})^{2k+1}}{2k+1}\right]^2. \end{aligned} \quad \text{(C.6)}$$

After some manipulations and making use of known series sums [22], (C.6) becomes (C.7)

$$\begin{aligned} c_n = \frac{1}{n!(n+1)!}\left[\sqrt{\pi\cdot\gamma}\cdot\left(\frac{(2n)!}{2^{2n+1}\cdot n!} - \frac{R_{0,n}}{4}\,\mathrm{erf}\,(\sqrt{\gamma})\right)\right. \\ \left.+\gamma\cdot e^{-\gamma}\cdot\left(\frac{R_{0,n}}{2} - \sum_{i=0}^{n-2} d_{i,n}\cdot\gamma^{i+1}\right)\right]^2 \end{aligned} \quad \text{(C.7)}$$

with $R_{0,n}$ simply obtained by (C.5) and expressed by (C.8) and the $d_{i,n}$ coefficients that are expressed by (C.9)

$$\begin{aligned} R_{0,n} &= P_n\left(-\frac{3}{2}\right) \\ &= \frac{(2n-1)!}{2^{2(n-1)}\cdot(n-1)!} \\ &= \frac{(2n)!}{2^{2n-1}\cdot n!} \end{aligned} \tag{C.8}$$

$$d_{i,n} = \frac{1}{i!}\sum_{p=i}^{n-2} q_{p,n}\cdot\left[\sum_{m=1}^{i}(-1)^m\binom{i}{m}m^p\right]. \tag{C.9}$$

Now, we need to make coefficient $q_{p,n}$ of $Q_n(k)$ explicit as a function of coefficient $p_{i,j}$ of $P_n(k)$.

From (C.5), it is possible to write (C.10)

$$\begin{aligned} R_{0,n} &= P_n(k) - (2k+3)Q_n(k) \\ &= \sum_{i=0}^{n-1} p_{i,m}k^i - (2k+3)\cdot\sum_{i=0}^{n-2} q_{i,n}k^i \\ &= (p_{0,n} = 3q_{0,n}) + \sum_{i=1}^{n-2}(p_{i,n} - 2q_{i-1,n} - 3q_{i,n}) \\ &\quad\cdot k^i + (p_{n-1,n} - 2q_{n-2,n}) \end{aligned} \tag{C.10}$$

by which it is evident that

$$\begin{aligned} p_{n-1,n} - 2q_{n-2,n} &= 0, \qquad i = n-1 \\ p_{i,n} - 2q_{i-1,m} - 3q_{i,n} &= 0, \qquad i = 1,\cdots,n-2 \\ p_{0,n} - 3q_{0,n} &= R_{0,n}, \qquad i = 0. \end{aligned} \tag{C.11}$$

As a consequence, the $q_{i,n}$ coefficients are recursively obtained by

$$\begin{aligned} q_{0,n} &= \frac{1}{3}(p_{0,n} - R_{0,n}), \qquad i = 0 \\ q_{i,n} &= \frac{1}{3}(p_{i,n} - 2q_{i-1,n}) - 3q_{i,n}, \qquad i = 1,\cdots,n-2 \\ q_{n-2,n} &= \frac{1}{2}p_{n-1,n}, \qquad i = n-1. \end{aligned} \tag{C.12}$$

The $p_{i,j}$ coefficient of $P_n(k)$ can also be recursively calculated making use of the definition in (C.4)

$$\begin{aligned} P_n(k) &= (k+3)(k+4)\cdot(k+n+1) \\ &= P_{n-1}(k)\cdot(k+n+1) \end{aligned} \tag{C.13}$$

which can be exploited to obtain (C.14). The identity in (C.14) allows us to obtain the recursive expression for the $p_{i,j}$ coefficient as expressed by (C.15).

$$\begin{aligned} \sum_{i=0}^{n-1} p_{i,n}k^i &= (k+n+1)\sum_{i=0}^{n-2} p_{i,n-1}k^i \\ &= p_{0,n} + \sum_{i=1}^{n-2} p_{i,n}k^i + p_{n-1,n}k^{n-1} \\ &= (n+1)p_{0,n-1} + \sum_{i=1}^{n-2}[p_{i-1,n-1} \\ &\quad + (n+1)p_{,n-1}]k^i + p_{n-2,n-1}k^{n-1} \end{aligned} \tag{C.14}$$

$$\begin{aligned} p_{n-1,n} &= p_{n-2,n-1}, \qquad i = n-1 \\ p_{i,n} &= p_{i-1,n-1} + (n+1)\cdot p_{i,n-1}, \\ &\qquad i = 1,\cdots,n-2 \\ p_{0,n} &= (n+1)\cdot p_{0,n-1}, \qquad i = 0. \end{aligned} \tag{C.15}$$

It is clear from (C.13) that

$$\begin{aligned} p_{n-1,n} &= 1 \qquad \forall n \\ p_{0,n} &= 3\cdot 4\cdot 5\cdots(n+1) = \frac{(N+1)!}{2} \qquad \forall n \end{aligned} \tag{C.16}$$

and by the combination of (C.15), (C.16), (C.12), and (C.7)–(C.9), the recursive algorithm of Section II for the c_n coefficient calculation is obtained.

The c_n values for $n = 0, 1$ are obtained in an analogous way from expression (C.3).

Appendix D
Noise Power on the Kth Carrier

The receiver input in the time-domain after A/D conversion is expressed by

$$\begin{aligned} s_r(mT_s) &= s_u(mT_s) + n_d(mT_s) + n_r(mT_s) \\ &= \alpha\cdot s(mT_s) + n(mT_s). \end{aligned} \tag{D.1}$$

The received symbol on the kth carrier after the DFT processing (see Fig. 1) is expressed by (D.2) by means of (14) and (16).

$$\begin{aligned} z_r[k] &= \sum_{m=0}^{L_{\text{fft}}-1} s_r[m]e^{-(2\pi/L_{\text{fft}})mk} \\ &= \alpha\sum_{m=0}^{L_{\text{fft}}-1} s[m]e^{-(2\pi/L_{\text{fft}})mk} + \sum_{m=0}^{L_{\text{fft}}-1} n[m]e^{-(2\pi/L_{\text{fft}})mk} \\ &= \alpha z[k] + e_n[k]. \end{aligned} \tag{D.2}$$

The power of the error contribution $e_n[k]$ is expressed by

$$\begin{aligned} P_{e_n}[k] &= e\{e_n[k]e_n^*[k]\} \\ &= \left\{\sum_{m=0}^{L_{\text{fft}}-1} n[m]e^{-(2\pi/L_{\text{fft}})mk}\sum_{p=0}^{L_{\text{fft}}-1} n^*[p]e^{j(2\pi/L_{\text{fft}})pk}\right\} \\ &= \sum_{p=0}^{L_{\text{fft}}-1}\left[\sum_{m=0}^{L_{\text{fft}}-1} E\{n[m]n^*[p]\}e^{-(2\pi/L_{\text{fft}})mk}\right] \\ &\quad\cdot e^{-(2\pi/L_{\text{fft}})pk} \\ &= \sum_{p=0}^{L_{\text{fft}}-1}\left[\sum_{m=0}^{L_{\text{fft}}-1} R_{nn}^*[m-p]e^{-(2\pi/L_{\text{fft}})mk}\right] \\ &\quad\cdot e^{j(2\pi/L_{\text{fft}})pk} \\ &= \sum_{p=0}^{L_{\text{fft}}-1}[S_{nn}[-k]\cdot e^{-(2\pi/L_{\text{fft}})p(-k)}]^*\cdot e^{j(2\pi/L_{\text{fft}})pk} \\ &= \sum_{p=0}^{L_{\text{fft}}-1} S_{nn}[k] \\ &= L_{\text{act}}S_{nn}\left(\frac{k}{T_b}\right) \\ &= L_{\text{act}}S_{n_dn_d}\left(\frac{k}{T_b}\right) + L_{\text{act}}S_{n_rn_r}\left(\frac{k}{T_b}\right) \end{aligned} \tag{D.3}$$

where $S_{nn}[\cdot]$ is the discrete PSD, $S_{nn}(\cdot)$ the continuous PSD of the noise contribution, and $L_{\text{act}} \leq L_{\text{fft}}$ are the active carriers obtained by the difference between the L_{fft} size and the number of the switched-off carriers which constitute the guard-band of the OFDM system.

REFERENCES

[1] *Asymmetric digital subscriber line (ADSL) metallic interface*, ANSI T1.413, 1995.

[2] *Radio broadcast systems; Digital audio broadcasting (DAB) to mobile, portable and fixed receivers.*, Final Draft prETS 300 401, Nov. 1994.

[3] *Framing structure, channel coding and modulation for digital terrestrial television*, DVB Document A012, June 1996.

[4] N. M. Blachman, "Bandpass nonlinearities," *IEEE Trans. Inform. Theory*, vol. IT-10, pp. 162–164, Apr. 1964.

[5] N. M. Blachman, "The output signals and noise from a nonlinearity with amplitude-dependent phase shift," *IEEE Trans. Inform. Theory*, vol. IT-25, pp. 77–79, Jan. 1979.

[6] O. Shimbo, "Effects of intermodulation, AM-PM conversion and additive noise in multicarrier TWT systems," *Proc. IEEE*, vol. 59, pp. 230–238, Feb. 1971.

[7] J. C. Fuenzalida, O. Shimbo, and W. L. Cook, "The domain analysis of intermodulation effects caused by non linear amplifiers," *COMSAT Tech. Rev.*, vol. 3, no. 1, 1973.

[8] H. E. Rowe, "Memoryless nonlinearities with Gaussian inputs: Elementary results," *Bell Syst. Tech. J.*, vol. 61, no. 7, pp. 1520–1523, Sept. 1982.

[9] J. Minkoff, "The role of AM-to-PM conversion in memoryless nonlinear systems," *IEEE Trans. Commun.*, vol. COM-33, pp. 139–143, Feb. 1985.

[10] B. Levine, *Fondements theoriques de la radiotechnique statistique*. New York: Editions de Moscou, 1973.

[11] W. B. Davenport and W. L. Root, *An Introduction to the Theory of Random Signals and Noise*. New YorK: McGraw-Hill, 1958.

[12] A. Papoulis, *Probability, Random Variables and Stochastic Process*, 3rd ed. New York: McGraw-Hill, 1991, p. 307.

[13] L. Cimini, "Analysis and simulation of a digital mobile channel using orthogonal frequency division multiplexing," *IEEE Trans. Commun.*, vol. COMM-33, pp. 665–675, 1985.

[14] G. Santella and F. Mazzenga, "A model for performance evaluation in M-QAM-OFDM schemes in presence of nonlinear distortions," in *Proc. IEEE Vehicular Technology Conf. (VTC)*, Chicago, IL, July 1995, pp. 830–834.

[15] N. M. Blachman, "Detectors, bandpass nonlinearities, and their optimization: Inversion of the Chebyshev transform," *IEEE Trans. Inform. Theory*, vol. IT-17, pp. 398–404, July 1971.

[16] A. R. Kaye, D. A. George, and M. J. Eric, "Analysis and compensation of bandpass nonlinearities for communications," *IEEE Trans. Commun.*, vol. COM-20, pp. 965–972, Oct. 1972.

[17] "Behavioral modeling of narrowband microwave power amplifiers with application in simulating spectral regrowth," in *IEEE Int. Microwave Symp. Dig.*, vol. 3, 1996, pp. 1385–1388.

[18] G. Chrisikos and C. J. Clark *et al.*, "A nonlinear ARMA model for simulating power amplifiers," in *IEEE Int. Microwave Symp. Dig.*, vol. 2, 1998, pp. 733–736.

[19] A. Saleh, "Frequency-independent and frequency-dependent nonlinear models of TWT amplifiers," *IEEE Trans. Commun.*, vol. 29, pp. 1715–1720, Nov. 1981.

[20] S. Cacopardi, P. Banelli, F. Frescura, and G. Reali, "OM-DS-SS wireless LAN radio subsystem: Performance in clipping environment using measured channel delay profiles," in *IEEE GLOBECOM*, London, U.K., Nov. 1996, pp. 1897–1903.

[21] J. G. Proakis, *Digital Communications*, 3rd ed. New York: McGraw-Hill, 1995.

[22] A. P. Prudnikov, Yu. A. Brychkov, and O. I. Marichev, *Integrals and Series*. New York: Gordon and Breach, 1986.

[23] J. Rinne and M. Renfors, "The behavior of orthogonal frequency division multiplexing signals in amplitude limiting channel," in *Proc. IEEE Int. Conf. Communications (ICC)*, New Orleans, LA, 1994, pp. 381–385.

[24] R. O'Neill and L. B. Lopes, "Performance of amplitude limited multitone signals," in *Proc. IEEE Vehicular Technology Conf. (VTC)*, Stockholm, Sweden, June 1994, pp. 1675–1679.

[25] Q. Shi, "OFDM in bandpass nonlinearity," *IEEE Trans. Consumer Electron.*, vol. 42, pp. 253–258, Aug. 1996.

Paolo Banelli (S'90–M'99) was born in Perugia, Italy, on May 19, 1968. He received the Laurea degree in electronics engineering and the Ph.D.degree in telecommunications from the University of Perugia, Perugia, Italy, in 1993 and 1998, respectively.

Currently, he is an Assistant Professor with the Department of Electronic and Information Engineering at the University of Perugia. His research interests include nonlinear distortions, broadcasting, and mobile communications.

Saverio Cacopardi (M'83) was born in Torino, Italy, on October 23, 1941. He received the Laurea degree in electrical engineering from the University of Rome, Rome, Italy, in 1970.

From 1971 to 1975, he worked on PCM transmission and CATV at SIP (Italian Telephone Operating Company). In 1975, he joined the Electrical Communication Department at the University of Rome as an Assistant Professor. From 1979 to 1985, he was an Associate Professor of Electrical Communications at the University of Ancona. From 1986 to 1991, he was an Associate Professor of Radio Aids to Navigation at the University "La Sapienza," Rome, Itay. In 1991, he joined the University of Perugia where he is now an Full Professor of Electrical Communications. His current research interests include mobile communications, WLAN, and broadcasting.